Preparation and analysis of the oxygen-plasma-anodized film on Ge(111)

Preparation and analysis of the oxygen-plasma-anodized film on Ge(1 1 1)

Liu Chun-rong†, Xu Zheng‡ and Liu Ling§

† Department of Physics, Anhui University, Hefei, People's Republic of China
‡ Department of Materials, Tongji University, Shanghai, People's Republic of China
§ Institute of Solid State Physics, Academia Sinica, Hefei, People's Republic of China

Abstract. Anodization of a germanium surface was carried out successfully in a high-frequency (0.5 MHz) oxygen plasma. The refractive index of the oxygen-plasma-anodized (OPA) film on Ge(1 1 1) measured by a TP-83 type ellipsometer is generally 1.67 ± 0.01 ($\lambda = 6328$ Å), and the film thickness ranged from 300 to 6000 Å depending on growth conditions. Physical characterization using Auger electron, x-ray photoelectron and infrared absorption spectroscopies indicates that the OPA film grown at 330–550 °C is mainly made up of GeO_2 with a disordered network of Ge–O_4 tetrahedra. The infrared absorption peak of the stretching vibration of Ge–O bonds is at 870 cm^{-1} and the bond angle of Ge–O–Ge is 129°. The OPA film possesses excellent electrical properties. The fixed charge density near the interface between OPA film and Ge is of the order of 1×10^{11} cm^{-2} and the breakdown electrical field is about 1×10^{6} V cm^{-1}.

1. Introduction

A successful metal–insulator–semiconductor (MIS) structure on silicon is the direct result of the passivation properties of native oxides and nitrides. Ge and Si belong to the group IV elements, whose structure is the same as the diamond lattice. These similarities suggest that good native oxide and nitride films on Ge might also exhibit passivation properties and high interfacial quality. The mobility of carriers in Ge is greater than that in Si. Because of this, Ge has been suggested as an attractive candidate for low-temperature complementary metal–oxide–semiconductor (CMOS) elements (Crisman *et al* 1984). A native oxide can be grown on Si by the thermal oxidation method at ambient pressure (e.g. 1 atm), but it is difficult to form a native germanium dioxide film effectively under similar conditions. Recently, the oxidation of a germanium surface at high oxygen pressure (137–681 atm) was reported (Crisman *et al* 1982). Native oxides formed on Ge by wet chemical reactions were reported by Gregory *et al* (1988). Growth of native germanium oxynitride film on Ge has been reported by Hymes and Rosenberg (1988). The plasma anodization constant (31 Å V⁻¹) of germanium has been reported by O'Hanlon (1969). In this paper, plasma anodization of a single-crystal germanium surface, compositional analysis and the characteristic infrared absorption spectrum of oxygen-plasma-anodized (OPA) films on Ge are reported. The growth rate of the OPA
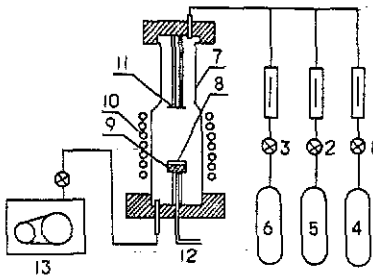
48% HF (2 min) and rinsed in deionized water. The wafer was placed on the anode holder in the reactor and the system was evacuated to 5 mTorr. The reactor was purged with pure oxygen. After 10 min purge, the oxygen pressure in the reactor was adjusted to 0.5–0.7 Torr by a needle valve (1) and the high-frequency furnace was turned on. When the sample temperature reached a suitable value (300–550 °C), the sample on the anode pedestal was biased at 10–150 V positive voltage with respect to the cathode for collecting electrons and negatively charged oxygen species. The OPA films of different thickness (from 300 to 6000 Å) on Ge may be formed by controlling the growth time and the anodising voltage.

Figure 2 shows a typical result for anodized films on Ge grown at 500 ± 10 °C and constant bias of 50 V. The variation of thickness with time was obtained by growing oxide films of different thickness on different slices for different anodization time. At longer time, parabolic behaviour is seen in figure 2, and can be represented by

$$X_t^2 - X_e^2 = kt \tag{1}$$

where X_e is the effective oxide thickness and X_t is the thickness after time t. The factor k is referred to as the parabolic rate constant.

The plasma anodic nitridation of OPA film on Ge can be performed by terminating the oxygen flow (turning off the needle valve 1) and introducing electronic-grade ammonia/ nitrogen (opening the valves 2 and 3) into the reactor at 520–630 °C. The nitrided film has better chemical stability in water.

3. Analysis of films

3.1. Refractive index and thickness

Refractive index and thickness of the OPA film on Ge were determined using a TP-83 type ellipsometer with microprograms made by the Beijing Information Optics Institute. The rotating polarizers are made of artificial polaroids and the indicator is of the null type. The wavelength of He–Ne laser illumination was 6328 Å. The ellipsometric parameters of two groups ($\psi_1, \Delta_1; \psi_2, \Delta_2$) were measured at two incidence angles of 70° and 75°, respectively. Refractive index and thickness of the transparent thin films on Ge may be determined by the ellipsometric parameters, the complex refractive index of germanium (Phillipp and Taft 1959) and the ellipsometric equations (Archer 1962) combined with a microprocessor (Apple-II computer). The precision of measuring thickness was about 10 Å.

The refractive index of OPA film on Ge is generally 1.67 ± 0.01, a value that coincides with that of vitreous GeO_2 (v-GeO_2). For the samples GeO-15 to GeO-20, the thickness of the OPA films ranges from 450 to 1330 Å (see figure 2).

3.2. Compositional analysis

The chemical composition of the OPA film on Ge was analysed by Auger electron spectroscopy (AES) and x-ray photoelectron spectroscopy (XPS) using a VG ESCA LAB
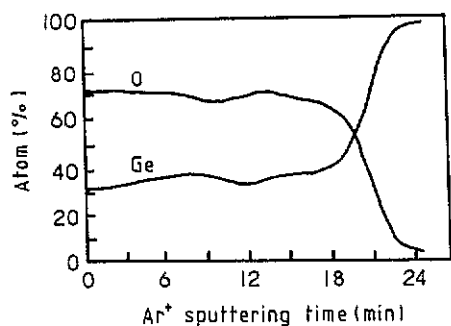
Figure 3. The chemical depth profile of the OPA film on Ge (sample GeO-3).
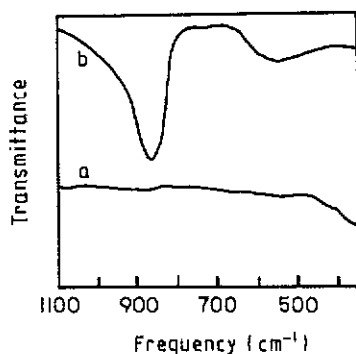

Figure 4. The transmittance of (a) blank germanium and (b) plasma-anodized film.

Mk-2 electron spectrometer. The surface concentration can be calculated in terms of the equation given by Chang *et al* (1975):

$$A_i = \alpha_i I_i \left(\sum_j \alpha_j I_j \right)^{-1} \tag{2}$$

where α_i are inverse Auger sensitivity factors. The running index j includes all the elements present in the oxide film. I_i is the Auger current determined from the peak-to-peak height of dN/dE type spectra. The electron escape depth influence upon the surface composition can be accounted for by

$$A_i(\eta) = \alpha_i I_i \eta_i^s \left(\sum_j \alpha_j I_j \eta_j^s \right)^{-1} \tag{3}$$

where the matrix term η also depends on the preferential sputtering and back-scattering contributions. In this work we shall evaluate η experimentally from a GeO_2 reference standard. The 's' indicates an arbitrarily chosen standard element on the sample surface, and it is one of the elements j. Finally, $A_i(\eta) \times 100$ is the composition in at.% from element i.

The quantitative calculation of AES for Ge–OPA film was carried out using equations (2) and (3). The principal Auger peak energy of Ge and O is 1137.5 and 507.0 eV, respectively. The AES of OPA film on Ge was measured using a primary electron of energy 5 keV and a beam current of 130 nA. The argon-ion energy used for sputtering was 5 keV, and the beam current was 14 nA. For the GeO-5 samples, the percentages of germanium and oxygen atoms on the surface are as follows:

$$A_{Ge}(\eta) = \alpha_{Ge} I_{Ge} \eta_{Ge}^O (\alpha_{Ge} I_{Ge} \eta_{Ge}^O + \alpha_O I_O \eta_O^O)^{-1} = 32.5\%$$

$$A_O(\eta) = 67.5\%.$$

The ratio of oxygen atoms to germanium atoms is 2.1, which is very close to the stoichiometry of GeO_2.

Figure 3 shows the chemical depth profile of the OPA film (sample GeO-3). It can be seen that the distribution of oxygen atoms and germanium atoms in the bulk of Ge–OPA film is more homogeneous.

The chemical states of the OPA film on Ge have been analysed by XPS with argon-ion sputtering. The target used was the Al K_α line (10 keV, 20 mA), and etching was carried

out using argon ions of energy 3 keV with beam current $20 \mu A$. The oxidation state of Ge(IV) was observed only on the surface of the OPA film (sample GeO-3). This result shows that all germanium atoms have been oxidized. There are double peaks of Ge(3d) in the XPS spectra after argon-ion sputtering for 5 and 10 min, respectively. The small peak on the side of lower energy near the principal peak (binding energy of 33.58 eV) is due to a few unoxidized germanium atoms, whose binding energy is about 29.20 eV (for details, see Liu and Liu 1989). The content of unoxidized Ge in the OPA film on Ge is less than that in the thermally grown germanium oxide film.

3.3. Infrared absorption spectrum

The transmittance of the OPA film on Ge(111) was measured by an IR-450S type infrared spectrophotometer (Shimadzu, Japan) in the range of 2.5–50 μm wavelength. Transmission of the polished and cleaned n-type germanium wafer (thickness 0.35 mm) was about 50% at room temperature (at a wavelength of 2.5–25 μm). In the range of 24–50 μm, there were several lattice vibration absorption bands in the IR spectra of Ge. Trace a of figure 4 is the IR transmission of the blank germanium wafer. Trace b shows the IR transmission of plasma-anodized film (thickness 0.62 μm) on Ge measured by the difference spectrum method (Liu and Liu 1988). Two IR absorption bands are observed at 870 and 560 cm^{-1}, respectively. The stronger band at 870 cm^{-1} is attributed to the stretching vibration of Ge–O bonds in the amorphous OPA film on Ge (confirmed by x-ray diffraction), whose full width at half-maximum is about 83 cm^{-1}. The weaker band (560 cm^{-1}) is due to vibration of Ge–Ge bonds in the OPA film. The stretching vibration constant α (439 N m^{-1}) and Ge–O–Ge bond angle θ (129°) have been calculated from IR absorption data together with the edges of vibration bands predicted by the centre-force-network model of Sen and Thorpe (1977).

The characteristic IR absorption spectrum for the OPA film on Ge is similar to that of v-GeO$_2$, which shows the similarities of the OPA film and v-GeO$_2$ in the short-range structure.

The result measured by a Nicolet 170 SX type Fourier-transform infrared spectrometer is the same as that mentioned above.

3.4. Capacitance–voltage characteristic

For the electrical measurements, several samples of Ge–MOS structures have been prepared by evaporating an ohmic contact (Au) on the back of a Ge wafer and aluminium dots (0.6 mm in diameter) on the OPA film. The C–V characteristics of the Ge–MOS structures were measured by a CTG-1 type high-frequency C–V characteristic instrument and plotted by an x–y recorder of JD-3 type. The experimental results show that a homogeneous and amorphous OPA film on Ge has an onset for destructive breakdown at a field of the order of 10^6 V cm^{-1}, and that the fixed charge density near the OPA film–Ge interface is about 10^{11} cm^{-2}. Although the OPA films have excellent electrical properties, they are highly soluble in water. For example, the OPA film with 3240 Å thickness was dissolved at room temperature in 30 s. Both germanium oxynitride and germanium nitride films are insoluble in water and resistant to atmospheric moisture.

Therefore, a device relying on such a native oxide film for operation characteristics can be protected by plasma anodic nitridation of the oxidized film on Ge.

4. Discussion

4.1. Growth rate

It is reported that the microscopic mechanism of oxygen transport during plasma anodization of Si involves short-range oxygen-ion migration in contrast to the case of high-temperature thermal oxidation. For a temperature of 25–600 °C, the contribution of a pure thermal process via diffusion of the neutral oxygen species is negligible compared to high-field-assisted oxygen-ion migration in the plasma anodization process (Perriere *et al* 1984). A similar result was also observed in the plasma anodization of Ge. The cathode and the sample on the anode holder are placed in the oxygen plasma region, and the negative oxygen ions were markedly attracted by the electrical field of anodization. Owing to the electrical field-enhanced transport, the migration coefficient of the ions in the oxide film is much greater than the usual diffusion coefficient in the absence of a field. Therefore, the plasma anodization rate is higher; for example, the OPA film on Ge grown at 125–301 °C for 30 min has a thickness of 1240 Å (sample GeO-4). The thickness of the thermally oxidized GeO_2 film grown at 550 °C for 120 min is only 630 Å.

The dependence of Ge–OPA film thickness X_f on anodization time t observed in our experiment is very similar to that found in the plasma anodization of Si (Kiermasz *et al* 1983). At longer time of anodization, a parabolic relationship is seen from figure 2. The parabolic rate constant k of the OPA film grown on Ge is about $3.1 \times 10^{-18} \, \mathrm{m^2 \, s^{-1}}$ under our experimental conditions (see section 2). In this parabolic region of growth, the anodization process is limited by the drift of ions through the oxide.

Our experiments also show that if the leakage current of oxygen ions is generated outside the oxide sample on the anode holder, the oxygen plasma anodization will be unsuccessful.

4.2. Composition

The difference between the binding energy of $Ge(2P_{3/2})$ in GeO_2 and that of $Ge(2P_{3/2})$ in GeO is 1.3 eV. The XPS of $Ge(2P_{3/2})$ measured after argon-ion sputtering for 10 min shows that no detectable GeO is observed in the OPA film on Ge. As mentioned in section 3, the infrared characteristic absorption bands, the Ge–O–Ge bond angle and the Ge(3d) binding energy in the OPA film on Ge(111) are similar to those of v-GeO_2. From these results it is seen that the OPA film on Ge possesses fourfold coordination of oxygen to germanium atoms. This amorphous OPA film is made up of a disordered network with mainly the tetrahedral structure of Ge–O_4.

5. Conclusions

Uniform, native germanium oxide films were grown on Ge(111) successfully in a high-frequency oxygen plasma at 300–550 °C. The results analysed by ellipsometry, infrared absorption, Auger electron and x-ray photoelectron spectroscopies, and *C–V* characteristic of Ge–MOS structure indicate that the OPA film on Ge is similar to vitreous

GeO_2 in the short-range structure. The OPA film also possesses excellent insulating and interface properties.

References

Archer R J 1962 *J. Opt. Soc. Am.* **52** 970
Chang C C, Muraka S P, Kumar V and Qintana G 1975 *J. Appl. Phys.* **46** 4237
Crisman E E, Ercil Y M, Loferski J J and Stiles P J 1982 *J. Electrochem. Soc.* **129** 1345
Crisman E E, Gregory O J and Stiles P J 1984 *J. Electrochem. Soc.* **131** 1896
Gregory O J, Pruit L A, Crisman E E, Roberts C and Stiles P J 1988 *J. Electrochem. Soc.* **135** 923
Hymes D J and Rosenberg J J 1988 *J. Electrochem. Soc.* **135** 961
Kiermasz A, Eccleston W and Moruzzi L 1983 *Solid-State Electron.* **26** 1167
Liu C R and Liu L 1988 *J. Phys. D: Appl. Phys.* **21** 799
—— 1989 *J. Phys. D: Appl. Phys.* **22** 1169
O'Hanlon J F 1969 *Appl. Phys. Lett.* **14** 127
Perriere J, Siejka J and Chang R H 1984 *J. Appl. Phys.* **56** 2716
Phillipp R H and Taft E A 1959 *Phys. Rev.* **113** 1002
Sen P N and Thorpe M F 1977 *Phys. Rev.* B **15** 4030
Sugano T and Mori Y 1974 *J. Electrochem. Soc.* **121** 113